the doublet is due to two (slightly inequivalent) ortho protons in the latter two complexes, whereas it stems from a single ortho proton in VO^{2+}–His. The line-width change is in agreement with the proposed structures of the complexes.

Future theoretical work may provide a better understanding of the factors that affect the magnitudes of the hyperfine and quadrupole splitting components. Then the measured parameters could serve to provide us with a more detailed picture of the geometric structure of VO^{2+}–Im complexes. However, even in the absence of a more rigorous quantitative analysis, the data presented here make it evident that ENDOR can be of great value in giving a semiquantitative insight into VO^{2+} binding site structure.

Acknowledgment is made to the donors of the Petroleum Research Fund, administered by the American Chemical Society, for support of this research. Financial support by the National Science Foundation (PRM-8100525, PCM-7903440) and Department of Energy (DE-AC02-81ER10911) for the purchase of equipment is gratefully acknowledged.

Registry No. $VO(Im)_4^{2+}$, 82871-04-3; $VO(H_2O)_5^{2+}$, 15391-95-4; L-histidine, 71-00-1; L-carnosine, 305-84-0; thiazole, 288-47-1.

Chlorite Oscillators: New Experimental Examples, Tristability, and Preliminary Classification[1]

Miklós Orbán,[2a] Christopher Dateo, Patrick De Kepper,[2b] and Irving R. Epstein*

Contribution from the Department of Chemistry, Brandeis University, Waltham, Massachusetts 02254. *Received March 16, 1982*

Abstract: Sustained oscillations are reported in the absorbance at 460 nm and in the potential of a Pt redox or iodide-sensitive electrode in a stirred-tank reactor (CSTR) containing solutions of chlorite, iodide, and an oxidizing substrate (IO_3^-, $Cr_2O_7^{2-}$, MnO_4^-, BrO_3^-) or chlorite, iodine, and a reducing substrate ($Fe(CN)_6^{4-}$, SO_3^{2-}, $S_2O_3^{2-}$). In addition to oscillations, a system containing chlorite, iodide, iodate, and arsenite can exhibit three different steady states, depending on initial conditions, for the same set of input flows, residence time, and temperature in the CSTR. Until a detailed mechanism for chlorite oscillators is developed, it seems reasonable to divide these systems into four classes: (A) the fundamental ClO_2^-–I^- (or ClO_2^-–I^-–IO_3^-) oscillator, (b) ClO_2^-–I^-–oxidant systems, (C) ClO_2^-–IO_3^- or (or I_2)–reductant systems, (D) iodine-free systems, e.g., ClO_2^-–$S_2O_3^{2-}$. A corresponding classification of bromate oscillators is discussed.

Oxyhalogen ions—bromate, iodate, or chlorite—are indispensable constituents of all known homogeneous isothermal chemical oscillators in solution. Although the first oscillating reaction discovered, the Bray–Liebhafsky reaction,[3] is an iodate system, the overwhelming majority of oscillators discovered to date contain either bromate or chlorite. The only other iodate oscillators developed since Bray's discovery in 1921 have been the related Briggs–Rauscher systems.[4,5]

Bromate oscillators have been by far the most thoroughly studied and characterized, notably the prototype Belousov–Zhabotinskii (BZ) system, which was discovered over 20 years ago.[6] Extensive bodies of experimental and theoretical work are now in remarkably good agreement[7] for the BZ reaction. Noyes[8] has recently formulated a generalized mechanism for bromate oscillators and has used this scheme to divide the known bromate oscillators into five distinct categories. While recent discoveries in this laboratory[1] have extended the range of bromate-driven oscillation beyond those categories treated by Noyes, the fundamental mechanism and notion of classification remain sound.

The study of chlorite oscillators is at a more primitive stage, since the first of these systems[9] was discovered only a year ago. However, progress has been remarkably swift, and the systematic classification and mechanistic description of chlorite oscillators now seem within reach. In this paper we report the discovery of several new chlorite-based oscillating reactions, summarize the

Table I. Chlorite Oscillators in a CSTR

no.	system	special features	ref
1	ClO_2^-–I^-	bistability between stationary and oscillating states	10
2	ClO_2^-–I^-–IO_3^-		this work
3	ClO_2^-–I^-–malonic acid	batch oscillation, spatial wave patterns	11
4	ClO_2^-–I^-–$Cr_2O_7^{2-}$		this work
5	ClO_2^-–I^-–MnO_4^-		this work
6	ClO_2^-–I^-–BrO_3^-	bistability between stationary and oscillating states	this work
7	ClO_2^-–IO_3^-–H_3AsO_3	first chlorite oscillator discovered	9
8a	ClO_2^-–IO_3^-–$Fe(CN)_6^{4-}$		13
8b	ClO_2^-–I_2–$Fe(CN)_6^{4-}$		this work
9a	ClO_2^-–IO_3^-–SO_3^{2-}		13
9b	ClO_2^-–I_2–SO_3^{2-}		this work
10a	ClO_2^-–IO_3^-–$S_2O_3^{2-}$	batch oscillation	11
10b	ClO_2^-–I_2–$S_2O_3^{2-}$		this work
11	ClO_2^-–IO_3^-–$CH_2O{\cdot}HSO_2$		13
12	ClO_2^-–IO_3^-–ascorbic acid		13
13	ClO_2^-–IO_3^-–I^-–malonic acid	batch oscillation	11
14	ClO_2^-–I^-–IO_3^-–H_3AsO_3	tristability	this work
15	ClO_2^-–$S_2O_3^{2-}$	first iodine-free chlorite oscillator	12

(1) Part 11 in the series Systematic Design of Chemical Oscillators. Part 10: Orbán, M.; De Kepper, P.; Epstein, I. R. *J. Am. Chem. Soc.* **1982**, *104*, 2657–2658.

(2) Permanent addresses: (a) Institute of Inorganic and Analytical Chemistry, L. Eötvös University, H-1443, Budapest, Hungary. (b) Centre de Recherche Paul Pascal, Domaine Universitaire, 33405 Talence, France.

(3) (a) Bray, W. C. *J. Am. Chem. Soc.* **1921**, *43*, 1262–1267. (b) Liebhafsky, H. A. *Ibid.* **1931**, *53*, 896–911.

(4) Briggs, T. C.; Rauscher, W. C. *J. Chem. Ed.* **1973**, *50*, 496.

(5) Cooke, D. O. *Int. J. Chem. Kinet.* **1980**, *12*, 683–698.

(6) Belousov, B. P. *Ref. Radiat. Med.* **1959**, *1958*, 145–147.

(7) Field, R. J.; Noyes, R. M. *Acc. Chem. Res.* **1977**, *10*, 214–221. Noyes, R. M.; Field, R. J. *Ibid.* **1977**, *10*, 273–280.

(8) Noyes, R. M. *J. Am. Chem. Soc.* **1980**, *102*, 4644–4649.

(9) De Kepper, P.; Epstein, I. R.; Kustin, K. *J. Am. Chem. Soc.* **1981**, *103*, 2133–2134 (Part 2).

0002-7863/82/1504-5911$01.25/0

known chlorite oscillators, and make a start toward a phenomenological classification of these systems according to their behavior relative to the prototype chlorite–iodide system.[10] A more detailed classification must await a mechanistic description of chlorite-based oscillation, which we are in the process of developing.

In Table I, we list the homogeneous oscillatory reactions discovered to date in which chlorite is a constituent. Most of these reactions undergo oscillation only in a stirred-tank reactor (CSTR) with input and output flows of reactants and products, though some as indicated show batch oscillation as well.[11] Experimental data on several of these systems will be reported for the first time in this paper. We note that with the single exception of the ClO_2^-–$S_2O_3^{2-}$ reaction (no. 15), which is discussed in detail elsewhere,[12] all of these systems contain one or more iodine species (IO_3^-, I_2, I^-) in addition to chlorite.

Since the ClO_2^-–I^- system (no. 1) alone generates oscillation, it is reasonable to ask whether systems containing chlorite, iodide, and an oxidizing agent (no. 2–6) are in fact different oscillators; i.e., do the additional oxidants promote oscillation, or are they merely perturbations of the chlorite–iodide oscillator. We shall seek an answer to this question by using the same type of analysis that led to the initial discovery of these oscillators. That is, we shall examine the phase diagram of the system and scrutinize how the regions of monostability, bistability, and oscillation shift and distort as the input flows of oxidizing species are varied.

In a similar vein, one may ask what role the reducing agent plays in the ClO_2^-–IO_3^- (or I_2)–reducing agent oscillators (no. 7–12).[13] While the failure to oscillate of the ClO_2^-–IO_3^- (I_2) reaction alone shows that the reducing agent is an essential part of the system, one may justifiably enquire whether the reducing agent does anything other than provide a source of I^- by its reaction with IO_3^- (I_2). If this is its only role, then these oscillators are little more than variants of the more fundamental ClO_2^-–I^- and ClO_2^-–I^-–IO_3^- systems.

Experimental Section

The flow experiments were carried out in two thermally regulated stirred-tank glass (Pyrex) flow reactors. Each reactor contains a free-liquid–air interface. The first of these (reactor A) has been described in detail elsewhere.[14] Reactor B differs from reactor A primarily in that reactor B is built into the sample chamber of a Beckmann 25 recording spectrophotometer. In either reactor, simultaneous measurements could be made of the absorbance of the solution and of the potentials of a platinum redox electrode (vs. $Hg|Hg_2SO_4|K_2SO_4$ reference) and/or an Orion iodide-specific electrode. Absorbances were generally measured at 460 nm, the wavelength of maximum I_2 absorbance. The path lengths were 4.05 and 3.4 cm in reactors A and B, respectively.

All experiments were carried out at 25.0 ± 0.1 °C. The constraints that were varied were the residence time τ (or flow rate $k_0 = 1/\tau$) and the concentrations $[A_i]_0$ that the input species A_i would reach in the reactor if no reaction were to occur. All solutions were prepared with doubly distilled water from high-purity commercially available grades of $NaClO_2$, KI, KIO_3, I_2, and other reagents. Chlorite solutions were stabilized by the addition of 0.001 M sodium hydroxide. Acetate or sulfate buffers of the appropriate pH were generated in situ as described earlier.[10]

Phase diagrams were determined by either of two methods. In the first approach, the potentiometric or spectrophotometric response of the system was followed as a function of flow rate at a fixed composition. The composition was then changed and the flow rate varied again. After a number of compositions had been investigated, we selected an appropriate flow rate at which to construct the constraint–constraint ($[X]_0$–$[Y]_0$) plot. A more rapid, though less thorough, approach employed in some cases consisted of choosing a fixed flow rate and then changing the reservoir compositions, allowing the system to reach a stationary or oscillating state before each reservoir change was made.

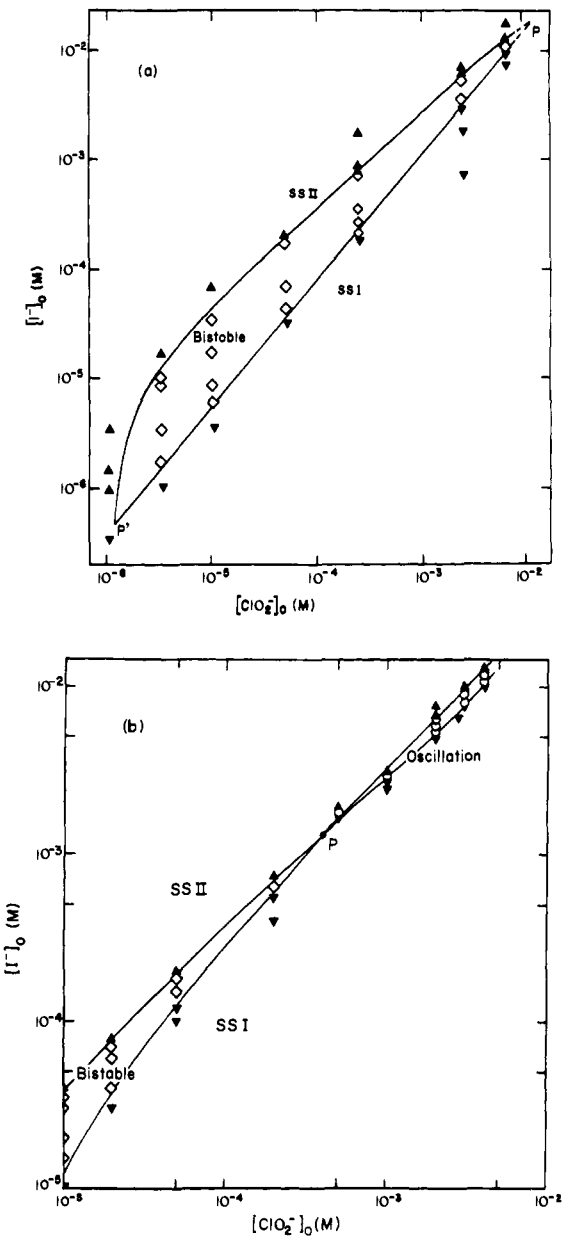

Figure 1. Two sections in the $[ClO_2^-]_0$–$[I^-]_0$ plane of the phase diagram for the chlorite–iodide system. Solid lines divide the regions of monostability (SS I, ▼; SS II, ▲), bistability (◊), and oscillation (○). Symbols show experimental points. Dashed line indicates region inaccessible experimentally because of iodine precipitation. P and P′ are cross points or critical points where the bistable region disappears as SS I and SS II coalesce. Constraints: (a) pH 3.35, $k_0 = 5.4 \times 10^{-3}$ s^{-1}, $T = 25$ °C; (b) pH 2.04, $k_0 = 1.1 \times 10^{-3}$ s^{-1}, $T = 25$ °C.

Phase Diagrams

Much of our analysis of these systems is based on the study of two types of graphs: the constraint–response plot and the phase diagram, which is a constraint–constraint plot. The constraint–response plot shows long-term behavior of a system (e.g., a stationary-state concentration or range of sustained concentration oscillations) as a function of a constraint (k_0 or an $[A_i]_0$). An example may be found in Figure 4 below. The phase diagram divides the constraint space into different regions according to the type of long-term behavior or phase (e.g., monostability, bistability, oscillation, chaos) shown by the system in response to the constraints. Two sections of the phase diagram for the chlorite–iodide system are shown in Figure 1. The regions of monostability of the two stationary steady states, SSI, characterized by low I^- and (when an oxidizing substrate is present) high

(10) Dateo, C. E.; Orbán, M.; De Kepper, P.; Epstein, I. R. *J. Am. Chem. Soc.* **1982**, *104*, 504–509 (Part 5).
(11) De Kepper, P.; Epstein, I. R.; Kustin, K.; Orbán, M. *J. Phys. Chem.* **1982**, *86*, 170–171 (Part 8).
(12) Orbán, M.; De Kepper, P.; Epstein, I. R. *J. Phys. Chem.* **1982**, *86*, 431–433 (Part 7).
(13) Orbán, M.; De Kepper, P.; Epstein, I. R.; Kustin, K. *Nature (London)* **1981**, *292*, 816–818 (Part 4).
(14) De Kepper, P.; Epstein, I. R.; Kustin, K. *J. Am. Chem. Soc.* **1981**, *103*, 6121–6127 (Part 3).

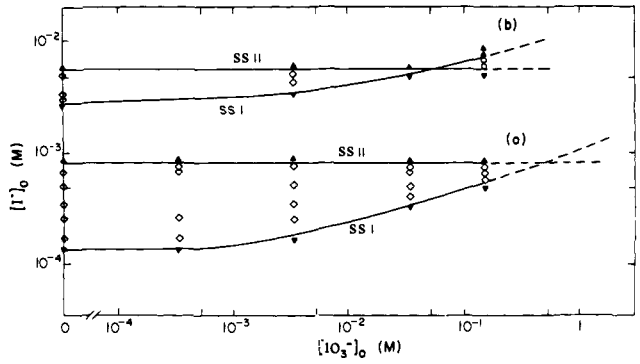

Figure 2. Two $[I^-]_0$–$[IO_3^-]_0$ sections of the phase diagram of the chlorite–iodide–iodate system. Fixed constraints as in Figure 1a: (a) $[ClO_2^-]_0 = 2.5 \times 10^{-4}$ M, (b) $[ClO_2^-]_0 = 2.5 \times 10^{-3}$ M. Symbols as in Figure 1. Dashed lines indicate limit of iodate solubility.

oxidant concentration, and SSII, with high $[I^-]$ and low [oxidant], are divided by regions of bistability (Figure 1a and 1b) and/or oscillation (Figure 1b).

Though easily obtainable from experiments in flow systems, these phase diagrams were not used until recently[15] as a source of information on the underlying mechanism and dynamics of a chemical system. Boissonade and De Kepper[16] have shown that systems possessing a particular kind of nonlinear dynamics exhibit a combination of bistable and oscillating domains resulting in a characteristic phase diagram like that of Figure 1b. In such systems, an intrinsically bistable subsystem, which shows hysteresis as a function of some constraint, is modified by a feedback species that acts to change the effective value of the constraint by a different amount on each of the two bistable branches. If relaxation to the steady states of the bistable subsystem is rapid compared with the time required for the establishment of the feedback effects, then the resulting phase diagram contains two different monostable regions, a bistable region, and an oscillatory region, all of which meet at a single "cross point".

In spite of the oversimplified model first used to derive the cross-shaped diagram, it has been found experimentally that a number of real systems, including the Belousov–Zhabotinskii[15a] and Briggs–Rauscher[16] reactions, exhibit this behavior. In fact, the chlorite oscillators were developed by seeking appropriate feedback species to couple with a bistable chlorite subsystem.

In asking whether a "new" chlorite oscillator contains anything more of dynamical significance than the prototype ClO_2^-–I^- system, we are enquiring whether the additional reactant species increases the size of the oscillatory region by creating a further differential feedback on the two branches. If so, then oscillations should occur at lower $[ClO_2^-]_0$ than in the chlorite–iodide system with the same other constraints (pH, residence time, temperature). The two solid lines in Figure 1 represent the boundaries of stability of the two steady states, and an increase in the differential feedback should shift the cross point to the left without shrinking the region of oscillation that exists at higher $[ClO_2^-]_0$.

Results

Detailed experimental results on the chlorite–iodide system, some of which are summarized in Figure 1, may be found in ref 10. Data on several other chlorite oscillators appear in the references given in Table I. We present in this section results on a number of oscillators not previously reported in the literature as well as a particularly interesting phase diagram for a variant of the first chlorite oscillator discovered, the chlorite–arsenite–iodate–iodide system.

Chlorite–Iodide–Iodate. Study of this system was undertaken in an attempt to simplify and to understand a variety of oscillators containing chlorite, iodate, and a reducing substrate.[9,13] The reductants in those studies were viewed as an indirect source of iodide, and we shall return to this point in the Discussion. Direct introduction of iodide did indeed generate oscillation. Figure 2 shows two sections of the phase diagram in the $[IO_3^-]_0$–$[I^-]_0$ constraint plane that differ only in their $[ClO_2^-]_0$ values. The flow rates and pH are the same as in Figure 1a for the chlorite–iodide system. We see that for the higher values of the chlorite flux, addition of iodate promotes oscillation by shifting the cross point to lower iodide and chlorite fluxes, making that point accessible before the onset of iodine precipitation.

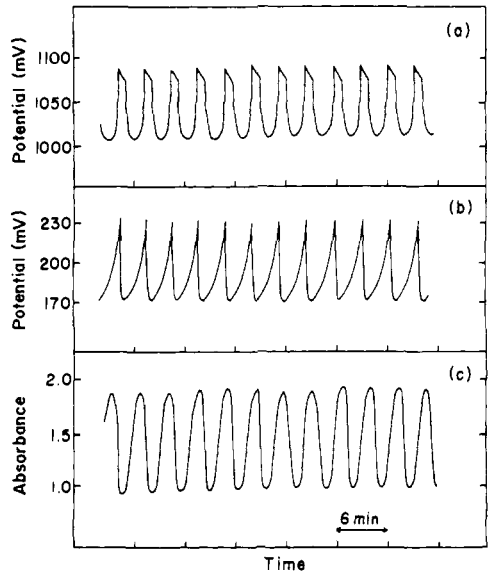

Figure 3. Oscillations in the potential of a platinum electrode (a) and an iodide-sensitive electrode (b) (relative to a standard hydrogen electrode) and in the optical density at 460 nm (c). Constraints: $[I^-]_0 = 0.0075$ M, $[ClO_2^-]_0 = 0.002$ M, $[BrO_3^-]_0 = 0.016$ M, pH 0.95, $T = 25$ °C, $k_0 = 4.6 \times 10^{-3}$ s^{-1}.

We see from Figure 2 that as $[IO_3^-]_0$ is increased, the region of bistability narrows. The high-iodide steady state (SSII) can be maintained only for increasingly high iodide inputs. On the other hand, the stability boundary of the low-iodide state (SSI) is unaffected by the addition of iodate. Thus iodate provides little or no feedback on SSI, while the shift of the stability boundary of SSII corresponds to a negative feedback on $[I^-]_0$ in SSII.

The width (range of $[I^-]_0$) of the bistable region shrinks as either $[ClO_2^-]_0$ or $[IO_3^-]_0$ is increased. However, the difference in response ($[I^-]_{ss}$) between the two states remains virtually constant. At high $[ClO_2^-]_0$ and $[IO_3^-]_0$, the cross point can be reached, i.e., oscillation appears (Figure 2b). At lower chlorite fluxes, as in Figure 2a, the iodate solubility limit ($[NaIO_3]_0 \sim 1.5 \times 10^{-1}$ M at 25 °C) prevents us from reaching the oscillatory region. However, we were able to obtain oscillations with the input flows and residence time of Figure 2a by raising the temperature to 35 °C. Oscillations occur in this system over a relatively wide range of pH, from about 2 to 3.5.

Chlorite–Iodide–Bromate. This system exhibits oscillation at a lower pH (<1.5) than does the chlorite–iodide–iodate reaction. We may think of this oscillator as derived from a nonoscillatory $[ClO_2^-]$–$[I^-]$ system. A composition of $[ClO_2^-]_0 = 0.002$ M and $[I^-]_0 = 0.01$ M gives rise to a single high-iodide steady state at all flow rates and pH's ($0.5 \leq$ pH ≤ 4.0) tested. Introduction of 0.016 M $[BrO_3^-]_0$ produces no change of state above pH 1.5. Below this pH, however, with added bromate, large amplitude (200–300 mV) oscillations appear in the potentials of both the platinum and iodide-sensitive electrodes when $k_0 < 3.2 \times 10^{-3}$ s^{-1}. A typical oscillatory trace is shown in Figure 3.

On further decreasing the pH to 0.8, a new feature of interest, a subcritical Hopf bifurcation (seen in Figure 4), emerges, with both a stationary and a sustained oscillating state stable over a wide range of flow rates (3.6×10^{-3} s$^{-1} \leq k_0 \leq 11.5 \times 10^{-3}$ s^{-1}). It is also worth noting that the bromate–chlorite reaction itself is autocatalytic and gives rise to bistability.[17]

(15) (a) De Kepper, P.; Boissonade, J. *J. Chem. Phys.* **1981**, *75*, 189–195. (b) De Kepper, P.; Epstein, I. R. *J. Am. Chem. Soc.* **1982**, *104*, 49–55.
(16) Boissonade, J.; De Kepper, P. *J. Phys. Chem.* **1980**, *84*, 501–506.

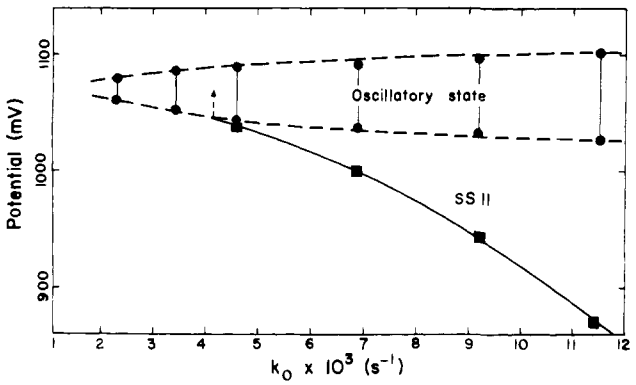

Figure 4. Potential of a Pt electrode (relative to standard hydrogen electrode) as a function of flow rate, showing bistability between a stationary and an oscillatory state. Vertical segments in the oscillatory state indicate the amplitude of oscillation. The arrow shows the spontaneous transition from the stationary to the oscillatory state. Fixed constraints: $[I^-]_0 = 0.01$ M, $[ClO_2^-]_0 = 0.002$ M, $[BrO_3^-]_0 = 0.016$ M, pH 0.8, $T = 25$ °C.

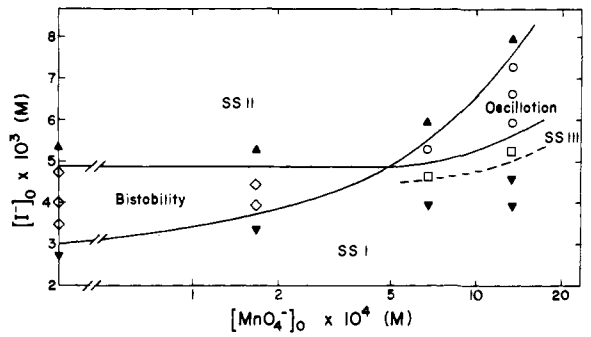

Figure 5. Section of the phase diagram of the chlorite–iodide–permanganate system in the $[I^-]_0$–$[MnO_4^-]_0$ plane: (▼) SS I, (▲) SSII, (◊) bistability SS I/SS II, (□) SS III, (○) oscillations. Fixed constraints: $[ClO_2^-]_0 = 2.5 \times 10^{-3}$ M, pH 3.5, $k_0 = 5.6 \times 10^{-3}$ s^{-1}, $T = 25$ °C.

Chlorite–Iodide–Permanganate. This system behaves in a manner similar to the chlorite–iodide–iodate system. Oscillations are observed at pH 3.5 and 2, but the system is monostable and fails to oscillate at pH 0.85 under all conditions tested. A phase diagram at pH 3.5 is shown in Figure 5. Note the strong similarity to the ClO_2^-–I^-–IO_3^- diagram of Figure 2. This reaction is seen to be even more complex than the chlorite–iodide–iodate system by the existence at the low $[I^-]_0$ end of the oscillating region of a third stationary state with an $[I^-]_{ss}$ intermediate between those of SSI and SSII. Lowering the pH shifts the oscillatory region to higher $[I^-]_0$. For example, at pH 2.05, oscillations are observed at a composition of $[I^-]_0 = 0.009$ M, $[ClO_2^-]_0 = 0.002$ M, $[MnO_4^-]_n = 0.001$ M for residence times ranging from 80 to 800 s. Increasing the MnO_4^- flux causes this range of residence times to narrow rapidly until the oscillating behavior vanishes completely.

Chlorite–Iodide–Dichromate. At pH <1.5, dichromate fluxes ranging from 1.4×10^{-3} M to 4.0×10^{-2} M induce oscillation at chlorite and iodide concentrations in regions where the system fails to oscillate in the absence of $Cr_2O_7^{2-}$ (e.g., $[ClO_2^-]_0 = 0.002$ M and $[I^-]_0 = 0.01$ M).

Chlorite–Iodide–Peroxydisulfate. The $S_2O_8^{2-}$ ion has a potential even greater than those of the other oxidizing substrates discussed above. However, addition of 0.002–0.04 M $[S_2O_8^{2-}]_0$ to the chlorite–iodide subsystem for $0.7 \le$ pH ≤ 2.0 produced no change in the observed region of oscillation. Thus it does not appear that this substrate enhances the ability of the system to oscillate.

Chlorite–Iodine–Thiosulfate. The chlorite–thiosulfate reaction constitutes the only known iodine-free chlorite oscillator.[12] It exhibits oscillation over a wide pH range (2–5) for $[ClO_2^-]_0$/$[S_2O_3^{2-}]_0$ ratios ranging from 0.7 to 1.5. However, at the nonoscillatory input composition $[ClO_2^-]_0 = 0.002$ M, $[S_2O_3^{2-}]_0 = 0.0033$ M, pH 2.3, it is found that the system can be caused to oscillate over a wide range of flow rates (6×10^{-4} $s^{-1} \le k_0 \le 1.2 \times 10^{-3}$ s^{-1}) by adding a flow of iodine, e.g., $[I_2]_0 = 0.0005$ M.

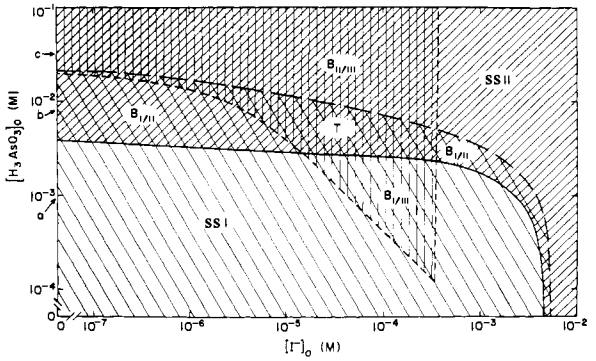

Figure 6. Section of the phase diagram of the chlorite–iodide–iodate–arsenite system showing tristability in the $[I^-]_0$–$[H_3AsO_3]_0$ plane. $B_{i/j}$ indicates region of bistability of SS_i and SS_j. T indicates region of tristability. Fixed constraints: $[ClO_2^-]_0 = 2.5 \times 10^{-3}$ M, $[IO_3^-]_0 = 2.5 \times 10^{-2}$ M, pH 3.35, $k_0 = 5.35 \times 10^{-3}$ s^{-1}, $T = 25$ °C. Arrows at a, b, and c indicate $[H_3AsO_3]_0$ values along which constraint–response plots in Figure 7 are made.

This system appears to constitute a more complex oscillator than the chlorite–thiosulfate reaction alone. From the observation that the optical density at 460 nm is zero during the oscillation, it follows that the I_2 must react rapidly with ClO_2^- and/or $S_2O_3^{2-}$. If it reacts only with chlorite, then the $[ClO_2^-]/[S_2O_3^{2-}]$ ratio would be shifted even further from the oscillatory range and chlorite–thiosulfate oscillations should not appear. On the other hand, if the iodine were to act simply to adjust the chlorite–thiosulfate ratio into the proper range by oxidizing $S_2O_3^{2-}$, a significant amount ($\sim 10^{-3}$ M) of I^- would be produced. We find, however, that no oscillation occurs in the ClO_2^-–$S_2O_3^{2-}$ system in the presence of 10^{-3} M iodide.

Chlorite–Iodine–Ferrocyanide. Like thiosulfate, ferrocyanide also produces oscillations when combined with chlorite and iodine. A composition of $[ClO_2^-]_0 = 0.002$ M, $[I_2]_0 = 0.0004$ M, $[Fe(CN)_6^{4-}]_0 = 0.0033$ M, pH 2.03, produces oscillation at $k_0 = 7 \times 10^{-3}$ s^{-1}. Again, if the only role of the $Fe(CN)_6^{4-}$ were to reduce iodine to iodide, the system would still be far outside the oscillatory region of the ClO_2^-–I^- system (cf. Figure 1b). This observation, along with differences in the wave form, amplitude, and frequency of oscillation, suggests that this system is somewhat more complex than the prototype ClO_2^-–I^- oscillator.

Chlorite–Iodine–Sulfite. Compositions in the neighborhood of $[ClO_2^-]_0 = 0.002$ M, $[I_2]_0 = 0.0004$ M, $[SO_3^{2-}]_0 = 0.005$ M, pH 2, $k_0 = 5 \times 10^{-4}$ s^{-1} showed oscillation, though no systematic study of this system was undertaken.

We note that in all the chlorite–iodine–reducing substrate systems studied, the flow of iodine necessary to generate oscillation is at least an order of magnitude less than the iodate flow required in the corresponding chlorite–iodate–substrate oscillator.

Chlorite–Iodide–Iodate–Arsenite. This system may be thought of as an arsenite perturbation of the chlorite–iodide–iodate system, as an iodide perturbation of the chlorite–iodate–arsenite oscillator, or as a hybrid of the chlorite–iodide and iodate–arsenite bistable subsystems. At constant temperature and pressure, the constraint space of the system is six-dimensional: the flow rate, pH, and the input concentrations of ClO_2^-, H_3AsO_3, I^-, and IO_3^- may be varied independently.

Several portions of the phase diagram have been described previously. The arsenite–iodate subsystem ($[ClO_2^-]_0 = [I^-]_0 = 0$) has been treated in detail in ref 14; it shows bistability but no oscillation. The chlorite–iodide subsystem ($[H_3AsO_3]_0 = [IO_3^-]_0 = 0$) was studied in ref 10; oscillations, bistability, and subcritical bifurcation were found. Oscillations and bistability in the chlorite–iodate–iodide subsystem ($[H_3AsO_3]_0 = 0$) were considered above.

(17) Epstein, I. R.; Dateo, C. E.; De Kepper, P.; Kustin, K.; Orbán, M. In "'Synergetics' Non-Linear Phenomena in Chemical Dynamics"; Pacault, A., Vidal, C., Eds.; Springer-Verlag: New York, 1981; p 188–191.

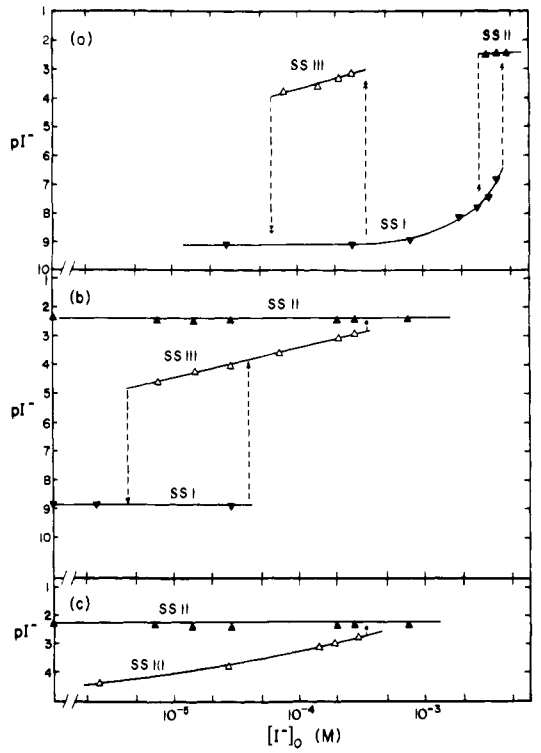

Figure 7. Constraint–response plots of steady-state $[I^-]$ vs. $[I^-]_0$ for three values of $[H_3AsO_3]_0$ on the phase diagram of Figure 6. Symbols: (▼) SS I, (▲) SS II, (△) SS III. Fixed constraints as in Figure 6. $[H_3AsO_3]$: 10^{-3} M (a), 8×10^{-3} M (b), 3.2×10^{-2} M (c).

The full system exhibits an extraordinary richness of behavior, even in the relatively small portion of the constraint space that we have been able to explore thus far. We first consider a section of the phase diagram (Figure 6) with all constraints except $[I^-]_0$ and $[H_3AsO_3]_0$ fixed at the same values as in Figure 2b and $[IO_3^-]_0 = 0.025$ M. In the absence of arsenite, the system shows a narrow region of bistability as a function of $[I^-]_0$, with hysteresis in the transitions between a low $[I^-]_{ss}$ steady state (SSI) and a high $[I^-]_{ss}$ steady state (SSII), as in Figure 2b. As $[H_3AsO_3]_0$ is increased, the stability boundaries of both states shift to lower $[I^-]_0$, and the relative width of the bistable region increases. At $[I^-]_0 < 5 \times 10^{-4}$ M, with the introduction of an arsenite flux of about 2×10^{-3} M, a new steady state (SSIII) appears, which has an intermediate value of $[I^-]_{ss}$ and a low $[I_2]_{ss}$. In various regions of the phase diagram we now see three different types of bistability (SSI/SSII, SSI/SSIII, SSII/SSIII), as well as a region in which any of the three states can exist, depending upon the initial conditions: *the system is tristable.*

The various types of multistability are illustrated in a different fashion in the constraint–response plot of Figure 7, where $[I^-]_{ss}$ is plotted as a function $[I^-]_0$ for three different values of $[H_3AsO_3]_0$ as indicated on the phase diagram of Figure 6. Note that only for the intermediate arsenite flux (Figure 7b) do we encounter the region of tristability.

While bistability is now a fairly well documented phenomenon, tristability is a rather novel occurrence in chemical systems. Only one other example has been reported.[18] It is an exceedingly difficult experimental task to identify and to characterize three or more different steady states of a single system. It is of critical importance to be able to measure as many different responses as possible; in this case we had three (redox potential, iodide-sensitive electrode potential, absorbance at 460 nm). Another useful clue in distinguishing the different states lies in their dynamic behavior. For example, when a jump perturbation is made in the flow rate, SSII shows excitability (large departure of concentrations from steady-state values before returning) while SSIII does not.

(18) De Kepper, P.; Pacault, A. *C. R. Hebd. Seances Acad. Sci., Ser. C* **1978**, *286*, 437–441.

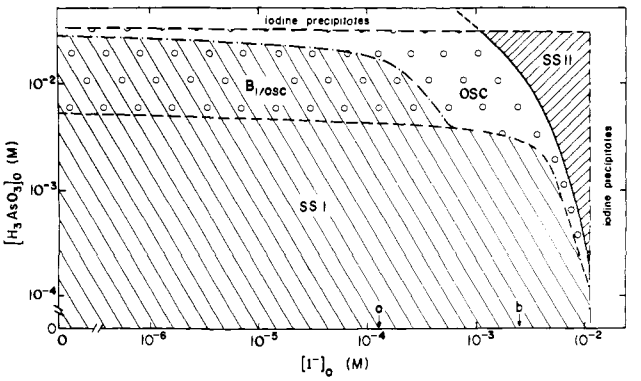

Figure 8. Section of the chlorite–iodide–iodate–arsenite phase diagram. All constraints and symbols as in Figure 6, except pH 2.0; area with circles represents the oscillatory state. Iodine precipitation occurs at $[I^-]_0 > 10^{-2}$ M or $[H_3AsO_3]_0 > 4 \times 10^{-2}$ M. Arrows at a and b indicate $[I^-]_0$ values along which constraint–response plots in Figure 9 are made.

In Figure 8 we show a section of the phase diagram with all constraints as in Figure 6 except that the pH is now 2.0 instead of 3.35. Here, as in several other chlorite systems, it is found that lowering the pH narrows the region of bistability, shifting the system toward an oscillatory domain. We note the absence of SSIII and the occurrence of relatively large regions of oscillation and of subcritical bifurcation, in which the initial conditions determine whether the system oscillates or resides in SSI. As in the previous example, the stability boundaries of both stationary states shift to lower $[I^-]_0$ as $[H_3AsO_3]_0$ is increased. Constraint–response plots of $[H_3AsO_3]_0$ vs. $[I^-]_{ss}$ for two values of $[I^-]_0$ are shown in Figure 9.

The data reported here represent the most complex phase diagram yet observed for a homogeneous liquid-phase reaction. We have, however, only begun to probe this and related systems. The existence of additional stationary and/or oscillatory states would not be surprising. Furthermore, although we primarily observed periodic oscillations, some aperiodic phenomena were also noted, though no systematic search for or analysis of this latter behavior was carried out. In this respect, the nonlinear dynamics of this system would seem to be at least as complex as those of the Belousov–Zhabotinskii reaction for which chemical chaos has been reported.[19]

Discussion

While we are still far from being able to present a full mechanistic treatment of chlorite oscillators, it may be helpful to consider, in Noyes' terminology,[8] the major "component stoichiometric processes" involved in chlorite–iodine oscillators. This consideration will enable us both to derive some understanding of the role of the various oxidizing and reducing substrates and to formulate a preliminary classification of chlorite oscillators. Also, each of the component processes has been studied individually, so constructing a mechanism for the oscillators may be largely a matter of "fitting together the pieces".

The major overall processes taking place in systems containing chlorite and iodide, iodine, and/or iodate appear to be[20]

$$I(V) + 5I^- \rightarrow 6I(0) \qquad (M1)$$

$$4I^- + Cl(III) \rightarrow 4I(0) + Cl^- \qquad (M2)$$

$$4I(0) + 5Cl(III) \rightarrow 4I(V) + 5Cl^- \qquad (M3)$$

where roman numerals in parentheses refer to oxidation states of iodine and chlorine, such as I(0) for $0.5I_2$ and Cl(III) for ClO_2^-. All three processes are strongly favored thermodynamically.

(19) Schmitz, R. A.; Graziani, K. R.; Hudson, J. L. *J. Chem. Phys.* **1977**, *67*, 3040–3044.

(20) At least at pH's above about 1, where decomposition of chlorite to ClO_2 is not significant (Gordon, G.; Kieffer, R. G.; Rosenblatt, D. H. *Prog. Inorg. Chem.* **1972**, *15*, 201–286).

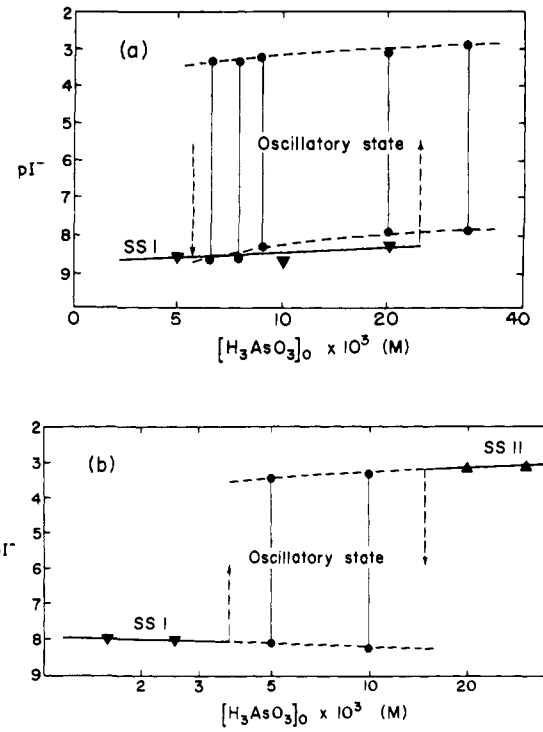

Figure 9. Constraint–response plots of steady-state $[I^-]$ vs. $[H_3AsO_3]_0$ for two values of $[I^-]_0$ on the phase diagram of Figure 8. Symbols: (▼) SS I, (▲) SS II. Vertical segments in the oscillating state indicate amplitude of the oscillation. Arrows show spontaneous transitions. $[I^-]_0$: 1.25×10^{-4} M (a), 2.5×10^{-3} M (b).

Reaction M1 is the Dushman reaction,[21] the kinetics of which have been determined by many investigators over the past 75 years. Although the data, which are summarized by Liebhafsky and Roe,[22] are not totally consistent, it does appear clear that the reaction is first order in iodide at low $[I^-]$ and second order at high $[I^-]$ ($\gtrsim 10^{-5}$ M). At least two mechanisms have been proposed.[22,23] Reaction M2 has been studied experimentally by Kern and Kim[24] and by De Meeus and Sigalla.[25] Rate laws were determined and agree on the fact that the reaction is autocatalytic in I_2 and inhibited by I^-. Again, two different mechanisms have been suggested. The third component process (eq M3) was the subject of a recent fast-kinetics study by Grant et al.[26] Those authors found a three-term rat e law and identified the major species likely to be responsible for each term. Thus, a fairly extensive body of experimental data and mechanistic speculation is available on these processes.

If, in addition to chlorite and iodide, a system contains an oxidizing substrate designated Ox, then the additional processes shown in (M4)–(M7) may occur:

$$Ox + I^- \rightarrow Red + I(0) \quad (M4)$$

$$5Ox + I(0) \rightarrow 5Red + I(V) \quad (M5)$$

$$Ox + Cl(III) \rightarrow Red + Cl(IV) \quad (M6)$$

$$2Ox + Cl(III) \rightarrow 2Red + Cl(V) \quad (M7)$$

where Red represents the reduced form of species Ox, and, for specificity, we have taken Ox to be a one-electron oxidant.

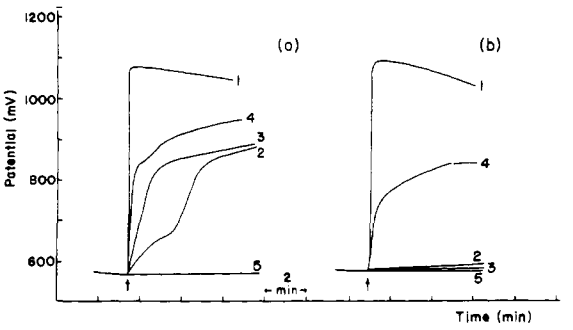

Figure 10. Redox potential (Pt electrode vs. SHE) vs. time for several oxyanion (Ox)–iodide batch reactions at pH 1 (a) and pH 2 (b). $[I^-] = 6.6 \times 10^{-4}$ M, $[Ox] = 3.3 \times 10^{-4}$ M. Arrows indicate start of the reaction, when acidic Ox solution was added to neutral I^- solution. Curves: (1) MnO_4^-, (2) BrO_3^-, (3) $Cr_2O_7^{2-}$, (4) IO_3^-, (5) $S_2O_8^{2-}$.

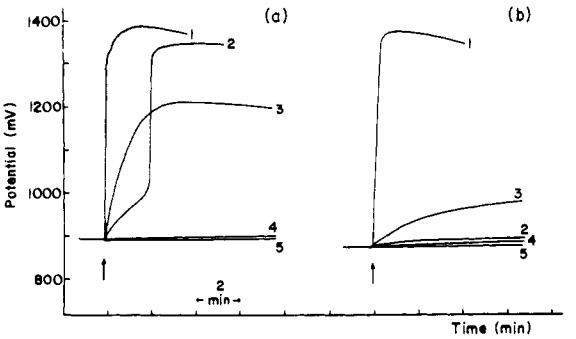

Figure 11. Redox potential (Pt electrode vs. SHE) vs. time for several oxyanion (Ox)–chlorite batch reactions at pH 1 (a) and pH 2 (b). $[ClO_2^-] = 4 \times 10^{-3}$ M, $[Ox] = 3.3 \times 10^{-3}$ M. Arrows indicate start of the reaction, when an acidic solution of Ox was added to a chlorite solution. Potential change due to ClO_2^-–acid interaction has been subtracted out. Curves: (1) MnO_4^-, (2) BrO_3^-, (3) $Cr_2O_7^{2-}$, (4) IO_3^-, (5) $S_2O_8^{2-}$.

Processes M4 and M5 complement processes M2 and M3, respectively, and if they proceed rapidly enough, should be able to induce oscillation, particularly where the $[ClO_2^-]_0/[I^-]_0$ ratio is too low for oscillation in the absence of Ox. Another way of viewing the effect of these processes is that they enhance the differential feedback on the bistable branches, thereby enabling the system to oscillate at lower $[ClO_2^-]_0$ than without added Ox. This low $[ClO_2^-]_0$ region is exactly where the oxidizing substrates of Table I are found to produce oscillation. On the other hand, processes M6 and M7 should consume chlorite, thereby, if sufficiently rapid, lessening the likelihood of oscillation.

A kinetic view of the above argument may be gleaned from Figures 10 and 11, which show the relative rates of reaction of five oxyanions with iodide and chlorite, respectively. We see in Figure 10 that process M4 occurs fairly rapidly for MnO_4^-, BrO_3^-, $Cr_2O_7^{2-}$, and IO_3^-, but only very slowly for $S_2O_8^{2-}$ at pH 1; at pH 2, only permanganate and iodate give significant rates of the (M4) reaction. Figure 11 shows that process M7 (or process M6) is very rapid for permanganate at either pH and proceeds at a noticeable though slower rate for bromate at pH 1 and for dichromate at pH 1 and 2. It is negligible for iodate and peroxydisulfate at both pHs and for bromate at pH 2.

We find that permanganate produces oscillation at pH 2–3.5 but not at pH 1, presumably because of the inhibitory effects of the rapid (M7) reaction (and/or because (M4) is much faster than (M2)). Bromate and dichromate both give oscillations at pH 1 but not at pH 2. Process M4 proceeds too slowly at the higher pH. Apparently (M7) is not rapid enough at pH 1 to interfere with the oscillatory dynamics. Iodate is a substrate that induces oscillation at both pHs because (M4) is rapid while (M7) is slow, while peroxydisulfate, in spite of its favorable potential, does not yield oscillation because (M4) is too slow at either pH.

In ClO_2^-–IO_3^-(or I_2)–Red systems, processes M1 and M2

(21) Dushman, S. J. *J. Phys. Chem.* **1904**, *8*, 453–481.
(22) Liebhafsky, H. A.; Roe, G. M. *Int. J. Chem. Kinet.* **1979**, *11*, 693–703.
(23) Morgan, K. J.; Peard, M. G.; Cullis, C. F. *J. Chem. Soc.* **1951**, 1865–1867.
(24) Kern, D. M.; Kim, C.-H. *J. Am. Chem. Soc.* **1965**, *87*, 5309–5313.
(25) De Meeus, J.; Sigalla, J. *J. Chim. Phys. Phys. Chim. Biol.* **1966**, *63*, 453–459.
(26) Part 9: Grant, J. L.; De Kepper, P.; Epstein, I. R.; Kustin, K.; Orbán, M. *Inorg. Chem.* **1982**, *21*, 2192–2196.

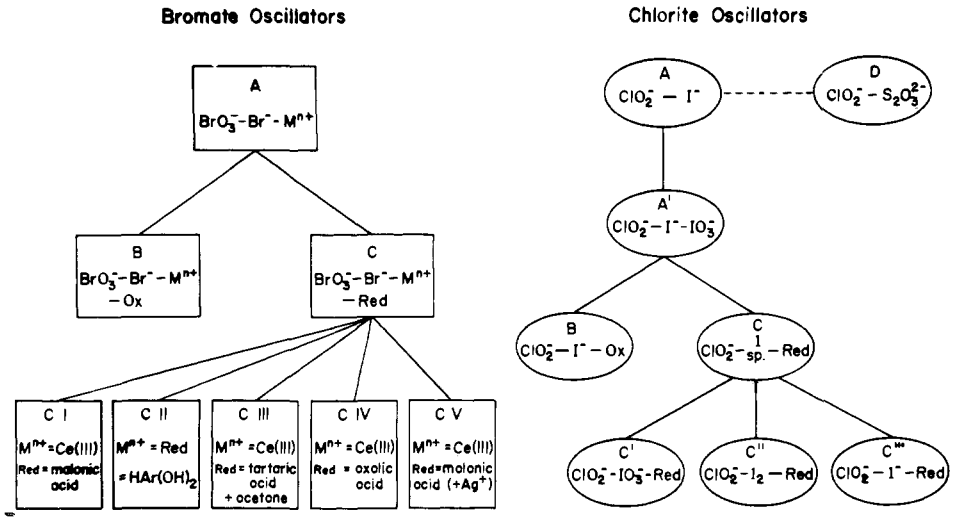

Figure 12. Schematic classification for bromate and chlorite oscillators. (I sp stands for iodine species).

cannot occur unless the reducing agent provides a source of iodide via sufficiently rapid processes M8 or M9:

$$I(V) + 6Red \rightarrow I^- + 6Ox \quad (M8)$$

$$I(0) + Red \rightarrow I^- + Ox \quad (M9)$$

Reactions such as (M10) will tend to inhibit oscillation or to shift

$$Cl(III) + 4Red \rightarrow Cl^- + 4Ox \quad (M10)$$

the oscillatory region to higher chlorite fluxes. It is of interest that in a study of ClO_2^-–IO_3^-–Red oscillators,[13] the authors note that arsenite reacts less rapidly with iodate (M8) than do the other substrates considered and that oscillation with arsenite as substrate must be induced by a single injection of I^- into the reactor.

On the basis of the above scheme, a simple preliminary classification of chlorite oscillators may be given. It is of course subject to improvement as further experimental work and a more detailed mechanism become available. The classification is as follows:

(A) Chlorite–Iodide. This is the fundamental or minimal chlorite–iodine oscillator in that it contains the minimal set of reactants necessary to generate processes M1–M3. It plays a role in the theory of chlorite–iodine oscillators similar to that of the recently discovered BrO_3^-–Br^-–catalyst minimal oscillator for bromate systems.[1]

(A') Chlorite–Iodide–Iodate. While this system fits into either categories B or C below, it may also be considered as a sort of fundamental oscillator that is generated (via (M4), (M8), or (M9)) by the systems of type B or C.

(B) Chlorite–Iodide–Oxidant. Several such systems, e.g., dichromate, bromate, and permanganate, have been discussed here, and there are almost certainly others. The chief requirements are that process M4 be rapid (but not faster than (M2) – (M3)) and that (M7) be slow in some accessible range of pH and reactant fluxes.

(C) Chlorite–Iodine Species–Reductant. Several subclasses may be distinguished within this category according to the oxidation number of the iodine species involved:

(C') Chlorite–Iodate–Reductant. A large number of these systems were treated in ref 13. Two other systems in this category, chlorite–iodate–malonic acid and chlorite–iodate–thiosulfate, are of special interest because they generate damped oscillation in a batch reactor.[11] Other reductants for which (M8) is fast and (M10) slow should also produce oscillation.

(C'') Chlorite–Iodine–Reductant. These systems, of which three examples were presented above, appear to be only minor variants of type C' in which (M9) replaces (M8).

(C''') Chlorite–Iodide–Reductant. The only example known of this type is the chlorite–iodide–malonic acid system, which is of special interest because it shows both batch oscillations and spatial wave patterns.[11] The slow decomposition of iodinated malonic acid species probably provides a long lasting, indirect flux of iodide (via (M2) and (M9)) in these systems.

(D) Chlorite–reductant. The only known non-iodine chlorite oscillator is chlorite–thiosulfate.[12] Since we are almost totally ignorant of how it functions, we place it for the moment in a category of its own. Further study may ultimately place it in an expanded category A. We also note that the ClO_2^-–IO_3^-–(I_2)–$S_2O_3^{2-}$ systems have connections to both categories C and D.

It is logical to compare our chlorite oscillator classification with the system devised by Noyes[8] for bromate oscillators. Our first attempts at such a comparison did not lead to useful insights until we recognized, aided by the discovery of the BrO_3^-–Br^-–catalyst oscillator,[1] that the five classes of bromate oscillators distinguished by Noyes constitute a subcategorization of a set of systems analogous to our category C (or, more precisely, C'''). That is, all the systems discussed by Noyes are of the type Br^-–BrO_3^-–M^{n+}–Red, where M^{n+} is a redox couple (a metal catalyst, except in the case of the Körös–Orbán[27] systems) and Red is an organic substrate that is oxidized by bromate. A schematic classification of bromate and chlorite oscillators is shown in Figure 12. While no bromate systems of class B have been reported, recent results[28] suggest that these oscillators do indeed exist.

It seems curious, at first sight, that while bromate oscillators have been studied for a much longer time and are far better understood mechanistically, the range of chlorite oscillators found experimentally is broader. Two factors, one chemical the other historical, account for this apparent paradox. From a chemical point of view, the fundamental bromate oscillator shows oscillation over an extremely narrow range of constraints,[1] while the ClO_2^-–I^- system oscillates under a relatively wide set of conditions.[10] This difference has made both the discovery and the development of new oscillators from the fundamental chlorite oscillator easier than in the bromate case. Also, chlorite oscillators were first developed in flow systems using a systematic procedure. In contrast, bromate oscillators were discovered accidentally in batch experiments and were thought of as batch systems. Since the number of systems that oscillate in batch is quite limited, it is only recently with the widespread application of flow techniques to bromate systems that the full range of bromate oscillators is beginning to appear.

Finally, we must recognize the rather primitive state of the classification scheme proposed for chlorite oscillators. The perception of finer distinctions within classes B and C as well as other refinements of our classification must await a deeper understanding of the component processes M1–M3, perhaps first in terms of a set of "pseudoelementary processes" resembling those identified

(27) (a) Körös, E.; Orbán, M. *Nature (London)* **1978**, *273*, 371–372. (b) Orbán, M.; Körös, E.; Noyes, R. M. *J. Phys. Chem.* **1979**, *83*, 3056–3057.
(28) De Kepper, P.; Alamgir, M.; Orbán, M.; Epstein, I. R., to be published.

by Noyes[8] in bromate oscillators. Development of even this level of mechanistic detail will surely involve the introduction of a number of intermediate species such as HOI and HIO_2 and probably such binuclear intermediates as $H_2I_2O_3$ and $ICIO_2$, for which there is already support in studies of the component processes.[21,24,25]

Acknowledgment. We thank Professor Kenneth Kustin for helpful discussions and a critical reading of the manuscript. This work was supported by Grant CHE7905911 from the National Science Foundation.

Registry No. ClO_2^-, 14988-27-7; I^-, 20461-54-5; IO_3^-, 15454-31-6; $Cr_2O_7^{2-}$, 13907-47-6; MnO_4^-, 14333-13-2; BrO_3^-, 15541-45-4; I_2, 7553-56-2; $Fe(CN)_6^{4-}$, 13408-63-4; SO_3^{2-}, 14265-45-3; $S_2O_3^{2-}$, 14383-50-7; H_3AsO_3, 36465-76-6.

Bistability in the Oxidation of Iron(II) by Nitric Acid[1]

Miklós Orbán[2] and Irving R. Epstein*

Contribution from the Department of Chemistry, Brandeis University, Waltham, Massachusetts 02254. *Received March 30, 1982*

Abstract: The autocatalytic reaction between ferrous ion and nitric acid has been studied at 25 °C in a continuous flow stirred tank reactor. The system exhibits bistability as a function of flow rate for a wide range of Fe(II) and HNO_3 input fluxes. The results obtained are in good agreement with a seven-step mechanism proposed earlier to account for the batch ferrous–nitric acid clock reaction. The possibility of constructing a chemical oscillator based on this system is discussed briefly.

Autocatalytic reactions in flow systems are of considerable interest because they may give rise to bistability or multistability, the existence of two or more *different* stable steady states of a system subject to the *same* set of imposed constraints. Which of the two states is attained in any particular experiment then depends only upon the past history of the system. This rather surprising behavior, which is possible only in an open chemical system, has been shown to be intimately related[3] to another fascinating phenomenon, chemical oscillation.

In the past year, a number of new bistable[4,5] and even tristable[1] systems have been developed starting from reactions previously known to be autocatalytic. Some of these systems have been further modified so as to produce oscillation.[4b,6] However, in contrast to the cerium bromate–bromide system studied earlier by Geiseler and Bar-Eli,[7] the autocatalytic reactions involved in these new systems have not been well enough understood mechanistically to allow a detailed comparison of calculated and experimental results.

In this paper, we present an experimental study of bistability in the autocatalytic oxidation of iron(II) by nitric acid in a stirred tank reactor (CSTR). An earlier investigation of this system under batch conditions combined with other work on related systems yielded a seven-step mechanism which gave excellent agreement with the observed behavior.[8] Here we use this mechanism to simulate the new flow experiments. Comparison of the results provides both a more stringent test of the mechanism and improved values for some of the free parameters in that scheme.

Table I. Reaction Scheme and Rate Expression Employed in Computer Simulations

no.	reaction and velocity	ref
P1	$Fe^{2+} + NO_3^- + 2H^+ = Fe^{3+} + NO_2 + H_2O$ $v_1 = 1.0 \times 10^{-7}\ M^{-1}\ s^{-1}[Fe^{2+}][NO_3^-]$ $v_{-1} = 1.4 \times 10^{-5}\ M\ s^{-1}[Fe^{3+}][NO_2]/[H^+]^2$	this work, 9, 10
P2	$Fe^{2+} + NO_2 + H^+ = Fe^{3+} + HNO_2$ $v_2 = 3.1 \times 10^4\ M^{-1}\ s^{-1}[Fe^{2+}][NO_2]$ $v_{-2} = 6.5 \times 10^{-4}\ s^{-1}[Fe^{3+}][HNO_2][H^+]$	9-11
P3	$Fe^{2+} + HNO_2 + H^+ = Fe^{3+} + NO + H_2O$ $v_3 = (7.8 \times 10^{-3}\ M^{-1}\ s^{-1} + 2.3 \times 10^{-1}\ M^{-2}\ s^{-1}[H^+] + 7.6 \times 10^{-3}\ M^{-1}\ s^{-1}[HNO_2]/[NO])[Fe^{2+}][HNO_2]$ $v_{-3} = (5.6 \times 10^{-4}\ s^{-1}[NO]/[H^+] + 1.6 \times 10^{-2}\ M^{-1}\ s^{-1}[NO] + 5.4 \times 10^{-4}\ s^{-1}[HNO_2]/[H^+])[Fe^{3+}]$	10-12
P4	$Fe^{2+} + NO = FeNO^{2+}$ $v_4 = 6.2 \times 10^5\ M^{-1}\ s^{-1}[Fe^{2+}][NO]$ $v_{-4} = 1.4 \times 10^3\ s^{-1}[FeNO^{2+}]$	13
P5	$2NO_2 + H_2O = HNO_2 + NO_3^- + H^+$ $v_5 = 1.0 \times 10^6\ M^{-1}\ s^{-1}[NO_2]^2$ $v_{-5} = 1.5 \times 10^{-2}\ M^{-2}\ s^{-1}[HNO_2][NO_3^-][H^+]$	9, 10
P6	$2HNO_2 = NO + NO_2 + H_2O$ $v_6 = 5.8\ M^{-1}\ s^{-1}[HNO_2]^2$ $v_{-6} = 2.0 \times 10^7\ M^{-1}\ s^{-1}[NO][NO_2]$	9, 10, 14
P7	$NO + NO_3^- + H^+ = NO_2 + HNO_2$ $v_7 = 5.0 \times 10^{-3}\ M^{-3}\ s^{-1}[NO_3^-][NO][H^+]^2$ $v_{-7} = 9.3\ M^{-2}\ s^{-1}[HNO_2][NO_2][H^+]$	this work, 9, 10

Experimental Section

Materials. High-purity $FeSO_4 \cdot 7H_2O$, HNO_3, and NO were available commercially. Nitric acid solutions were purged with N_2 for 1 h or more to remove dissolved gases. Ferrous solutions were freshly made for each experiment and were also purged with nitrogen. The NO used in the determination of the $FeNO^{2+}$ extinction coefficient was first passed through a 30-cm column of NaOH to remove any NO_2 present.

Reactor. The CSTR used has been described previously.[4a] However, it was found that the presence of oxygen and/or nitrogen oxides in the space between the liquid surface and the reactor cap impaired the reproducibility of the experiments. The reactor was then modified to eliminate this space so that the liquid completely filled the reactor volume of 28.6 cm^3. The reactor was thermostated at 25.0 ± 0.1 °C.

(1) Part 12 in the series Systematic Design of Chemical Oscillators. Part 11: Orbán, M.; Dateo, C.; De Kepper, P.; Epstein, I. R. *J. Am. Chem. Soc.*, preceding paper.

(2) Institute of Inorganic and Analytical Chemistry, L. Eötvös University, H-1443 Budapest, Hungary.

(3) Boissonade, J.; De Kepper, P. *J. Phys. Chem.* **1980**, *84*, 501-506.

(4) (a) De Kepper, P.; Epstein, I. R.; Kustin, K. *J. Am. Chem. Soc.* **1981**, *103*, 6121-6127. (b) Dateo, C. E.; Orbán, M.; De Kepper, P.; Epstein, I. R. *Ibid.* **1982**, *104*, 504-509. (c) Epstein, I. R.; Dateo, C. E.; De Kepper, P.; Kustin, K.; Orbán, M. In "Non-Linear Phenomena in Chemical Dynamics"; Vidal, C., Pacault, A., Eds.; Springer: New York, 1981; Vol. 12, pp 188-191.

(5) (a) Papsin, G. A.; Hanna, A.; Showalter, K. *J. Phys. Chem.* **1981**, *85*, 2575-2582. (b) Reckley, J. S.; Showalter, K. *J. Am. Chem. Soc.* **1981**, *103*, 7012-7013.

(6) (a) De Kepper, P.; Epstein, I. R.; Kustin, K. *J. Am. Chem. Soc.* **1981**, *103*, 2133-2134. (b) Orbán, M.; De Kepper, P.; Epstein, I. R.; Kustin, K. *Nature (London)*, **1981**, *292*, 816-818. (c) De Kepper, P.; Epstein, I. R.; Kustin, K.; Orbán, M. *J. Phys. Chem.* **1982**, *86*, 170-171. (d) Orbán, M.; De Kepper, P.; Epstein, I. R. *Ibid.* **1982**, *86*, 431-433.

(7) Geiseler, W.; Bar-Eli, K. *J. Phys. Chem.* **1981**, *85*, 908-914.

(8) Epstein, I. R.; Kustin, K.; Warshaw, L. J. *J. Am. Chem. Soc.* **1980**, *102*, 3751-3758.

0002-7863/82/1504-5918$01.25/0